

Electronic Supplementary Information

**Switching slow relaxation in a Mn^{III}₃Mn^{IV} cluster:
an example of grafting single-molecule magnets onto polyoxometalates**

Xikui Fang, Manfred Speldrich, Helmut Schilder, Rui Cao, Kevin P. O'Halloran, Craig L. Hill and Paul Kögerler

Synthesis of 2a: In a 100 mL beaker, a sample of 1·4H₂O·2CH₃COOH (0.21 g, 0.1 mmol) was suspended in a mixture of CH₃COOH (36 mL) and H₂O (24 mL). After vigorous stirring for 1 hr, solid Na₁₂[α -P₂W₁₅O₅₆]·18H₂O (0.86 g, 0.2 mmol) was then added to the above solution. After stirring for 1/2 hr at room temperature, the mixture was heated to 80 °C for another 1 hr and filtered. Dimethylamine hydrochloride (0.30 g) was then added to the solution. Any insoluble material precipitated overnight was removed by centrifugation. Slow evaporation of the dark red solution afforded dark red needle crystals (yield 0.23 g, 24.4% based on W). Elemental analysis, calcd. for C_{16.67}H_{85.67}Mn_{4.33}N_{5.33}O₈₁P₂W₁₅: C 4.24, H 1.83, N 1.58, Mn 5.05, P 1.31, W 58.5, Na, 0.0 %. Found: C 4.33, H 1.99, N 1.44, Mn 5.06, P 1.26, W 56.8, Na <0.02 %. Selected IR bands for **1** (KBr pellet, 2000–500 cm⁻¹): 1623(m), 1553(m), 1466(m), 1388(m), 1341(m), 1085(s), 1009(m), 944(s), 913(s), 801(vs, br), 711(s), 684(s), 625(m), 578(sh), 524(m).

Physical measurements: Infrared spectra (KBr pellets) were collected on a Bruker Tensor 27 instrument. Atmosphere compensation (CO₂ and H₂O) and baseline corrections (rubberband method) were carried out after spectrum collection. The ³¹P and ¹H NMR data were collected on a Varian VXR-400 MHz instrument (D₂O solutions). Typical sample concentrations were 0.2 – 0.5 mM. Elemental analysis results (ICP-OES) were obtained from Zentralabteilung für Chemische Analysen, Forschungszentrum Jülich GmbH, D-52425 Jülich, Germany.

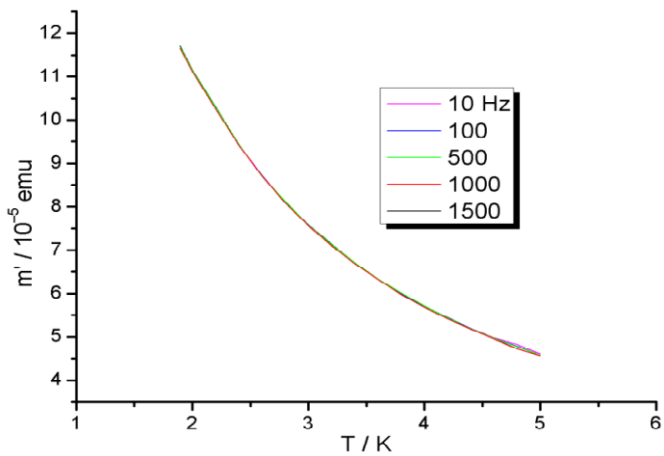


Figure S1. In-phase ac magnetization component m' of **2a** (24.06 mg) for frequencies ranging from 10 to 1500 Hz between 1.8 and 5 K in the absence of a dc bias field, illustrating the lack of frequency dependency. No out-of-phase component m'' is observed for the same parameter range.

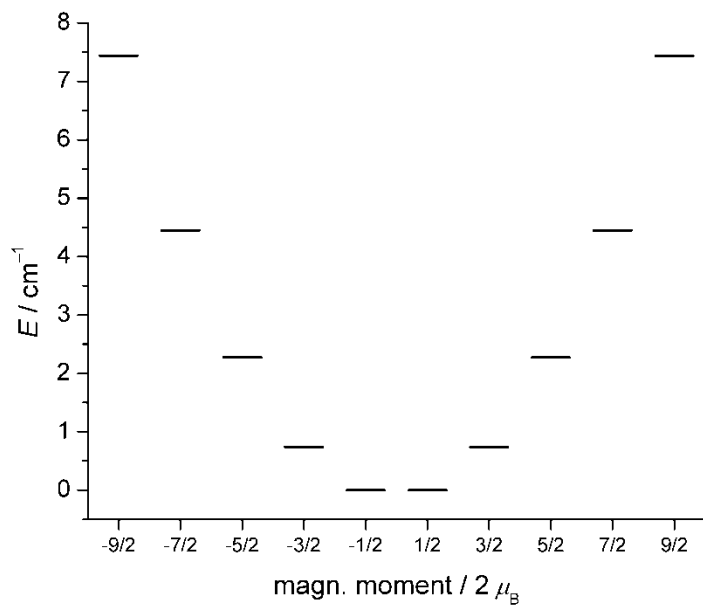


Figure S2. Calculated energies of the zero field-split substates belonging to the $S = 9/2$ ground state of **2a**.

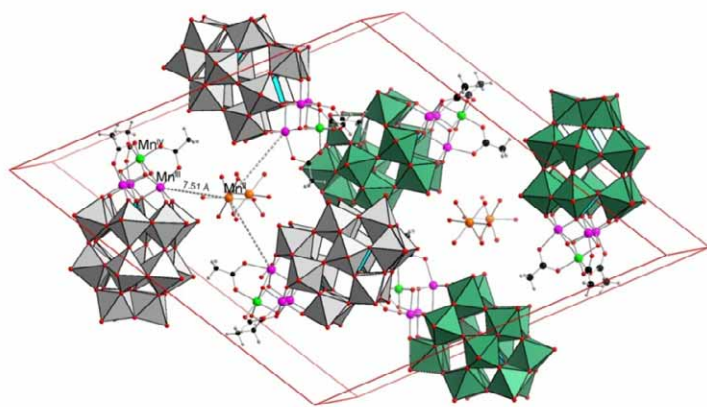


Figure S3. Arrangement of cluster anions in a unit cell of **2a**. Grey and green polyhedra distinguish the front and rear cluster trimers that are centered around Mn^{II} counter ions (orange spheres). The Mn^{II} ions are positioned on 6₃ axes and disordered equally over two positions related by a mirror plane. Compound **2a** crystallizes in space group *P*6₃/*m*.

Solution NMR results: ¹H NMR shows a single methyl resonance for the three acetate groups of **2** at 1.84 ppm, consistent with effective *C*_{3v} symmetry. ³¹P NMR, also as expected, only has a very broad signal at -11.9 ppm that attributed to the distal P atom, while the proximal P signal is too broadened to be observed due to its close proximity to the paramagnetic Mn centers, a situation that has been seen in other Mn-substituted Dawson systems (reference 3, see text).

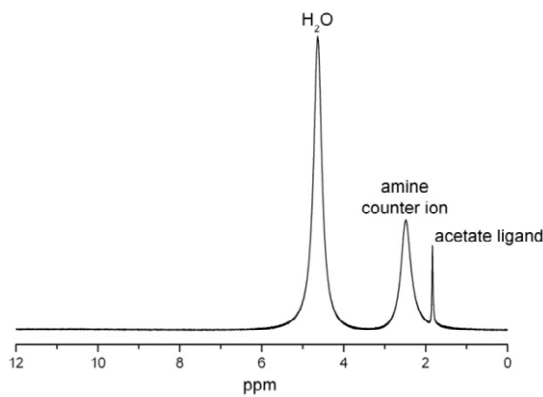


Figure S4. ¹H NMR spectrum of **2a** in D₂O.

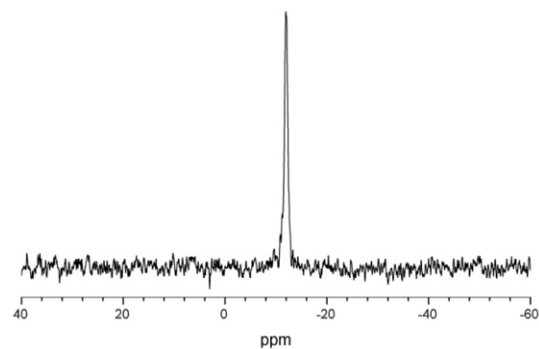


Figure S5. ^{31}P NMR spectrum of **2a** in D_2O .

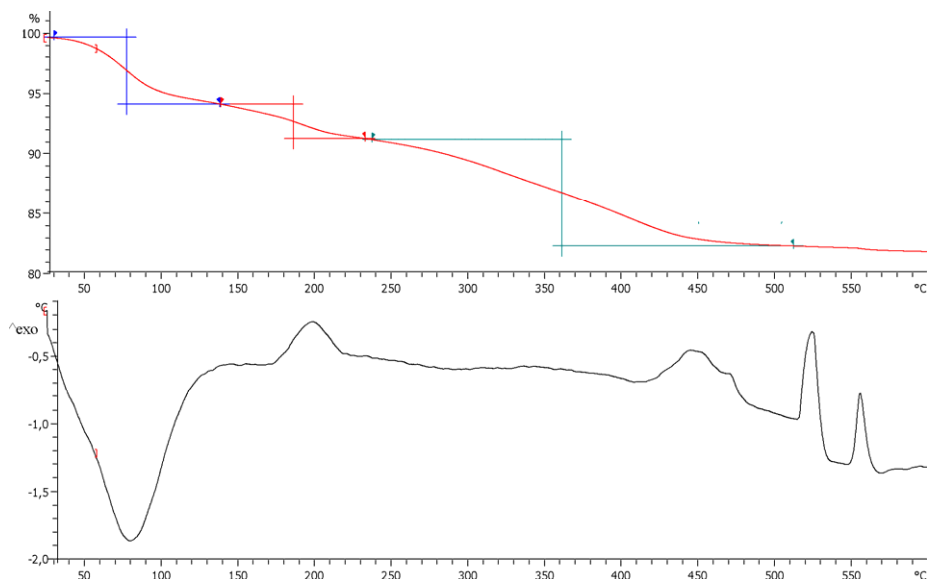


Figure S6. TGA and simultaneous DTA graphs of **2a** (10 K/min, 60 ml N_2 /min).

Magnetic simulations: Using our computational framework CONDON, we simulated the magnetic properties of **2a** based on all relevant influences on the molecular spin structure. Note that due to the inclusion of angular momentum contributions, the resulting magnetic states are not adequately characterized anymore by spin quantum numbers (e.g. S , m_S). In the case of **2a**, magnetic moments of single d³ and d⁴ ions are determined as a function of spin-orbit coupling, interelectronic repulsions, and ligand field effects, employing the full basis set of all microstates. The individual single-ion magnetic moments then are coupled to the molecular moment of the Mn^{III}₃Mn^{IV} cluster structure using a Heisenberg-type superexchange formalism as a function of an applied external field whereby all perturbations are taken into account simultaneously. Standard spectroscopic values are chosen for the spin-orbit coupling constant ζ (Mn^{IV}: $\zeta = 170 \text{ cm}^{-1}$; Mn^{III}: $\zeta = 190 \text{ cm}^{-1}$) and Racah parameters B (Mn^{IV}: $B = 700 \text{ cm}^{-1}$; Mn^{III}: $B = 800 \text{ cm}^{-1}$). The full Hamiltonian is defined as

$$\hat{H} = \underbrace{\sum_{i=1}^N \left[-\frac{\hbar^2}{2m_e} \nabla_i^2 + V(r_i) \right]}_{\hat{H}^{(0)}} + \underbrace{\sum_{i>j}^N \frac{e^2}{r_{ij}}}_{\hat{H}_{ee}} + \underbrace{\sum_{i=1}^N \zeta(r_i) \kappa \hat{l}_i \cdot \hat{s}_i}_{\hat{H}_{so}} + \underbrace{\sum_{i=1}^N \sum_{k=0}^{\infty} \left\{ B_0^k C_0^k(i) + \sum_{q=2}^k \left[B_q^k \left(C_{-q}^k(i) + (-1)^q C_q^k(i) \right) \right] \right\}}_{\hat{H}_{LF}} + \underbrace{\sum_{i=1}^N \mu_B (\kappa \hat{l}_i + 2 \hat{s}_i) \cdot \mathbf{B}}_{\hat{H}_{mag}}$$

and augmented by the Heisenberg exchange Hamilton (see text).